Double-heterostructure photonic crystal lasers with lower thresholds and higher slope efficiencies obtained by quantum well intermixing

Ling Lu*, Adam Mock, Mahmood Bagheri, Eui Hyun Hwang, John O'Brien and P. Daniel Dapkus

Department of Electrical Engineering - Electrophysics, University of Southern California
920 Downey Way, BHE 106, Los Angeles, California 90089, USA
lingl@usc.edu

Abstract: In order to reduce the optical absorption loss, an array of double-heterostructure photonic crystal microcavity lasers was fabricated in which much of the photonic crystal mirror region was disordered by quantum well intermixing. In characterizing these devices, we obtained more than a factor of two increase in slope efficiencies and more than 20% reduction in threshold pump powers compared to devices that were not intermixed.

OCIS codes: (140.5960) Semiconductor lasers; (130.3120) Integrated optics devices; (230.5298) Photonic crystals.

References and links

1. O. Painter, R. K. Lee, A. Scherer, A. Yariv, J. D. O'Brien, P. D. Dapkus, and I. Kim, "Two-dimensional photonic band-gap defect mode laser," Science **284**, 1819–1821 (1999).
2. H. G. Park, S. H. Kim, S. H. Kwon, Y. G. Ju, J. K. Yang, J. H. Baek, S. B. Kim, and Y. H. Lee, "Electrically driven single-cell photonic crystal laser," Science **305**, 1444–1447 (2004).
3. T. Yang, A. Mock, J. D. O'Brien, S. Lipson, and D. G. Deppe, "Edge-emitting photonic crystal double-heterostructure nanocavity lasers with InAs quantum dot active material," Opt. Lett. **32**, 1153–1155 (2007).
4. L. Lu, T. Yang, A. Mock, M. H. Shih, E. H. Hwang, M. Bagheri, A. Stapleton, S. Farrell, J. O'Brien, and P. D. Dapkus, "100 μW edge-emitting peak power from a photonic crystal double-heterostructure laser," Conference on Lasers and Electro-Optics (CLEO), Baltimore, Maryland, CMV3 (2007).
5. V. Aimez, J. Beauvais, J. Beerens, D. Morris, H. S. Lim, and B. S. Ooi, "Low-energy ion-implantation-induced quantum-well intermixing," IEEE J. Sel. Top. Quantum Electron. **8**, 870–879 (2002).
6. S. Charbonneau, E. S. Koteles, P. J. Poole, J. J. He, G. C. Aers, J. Haysom, M. Buchanan, Y. Feng, A. Delage, F. Yang, M. Davies, R. D. Goldberg, P. G. Piva, and I. V. Mitchell, "Photonic integrated circuits fabricated using ion implantation," IEEE J. Sel. Top. Quantum Electron. **4**, 772–793 (1998).
7. E. J. Skogen, J. W. Raring, G. B. Morrison, C. S. Wang, V. Lal, M. L. Masanovic, and L. A. Coldren, "Monolithically integrated active components: A quantum-well intermixing approach," IEEE J. Sel. Top. Quantum Electron. **11**, 343–355 (2005).
8. A. Mock, L. Lu, and J. D. O'Brien, "Spectral properties of photonic crystal double-heterostructure resonant cavities," Opt. Express **16**, 9391–9397 (2008).
9. B. S. Song, S. Noda, T. Asano, and Y. Akahane, "Ultra-high-Q photonic double-heterostructure nanocavity," Nat. Materials **4**, 207–210 (2005).
10. J. F. Ziegler, M. D. Ziegler, and J. P. Biersack, SRIM-2003 (2005).
11. M. H. Shih, W. Kuang, A. Mock, M. Bagheri, E. H. Hwang, J. D. O'Brien, and P. D. Dapkus, "High-quality-factor photonic crystal heterostructure laser," Appl. Phys. Lett. **89**, 101,104 (2006).
12. M. H. Shih, W. Kuang, T. Yang, M. Bagheri, Z. J. Wei, S. J. Choi, L. Lu, J. D. O'Brien, and P. D. Dapkus, "Experimental characterization of the optical loss of sapphire-bonded photonic crystal laser cavities," IEEE Photon. Technol. Lett. **18**, 535–537 (2006).

#101315 - $15.00 USD Received 9 Sep 2008; revised 8 Oct 2008; accepted 8 Oct 2008; published 14 Oct 2008

13. A. Mathur and P. D. Dapkus, "Fabrication, characterization and analysis of low threshold current density 1.55-mu m-strained quantum-well lasers," IEEE J. Quantum Electron. **32**, 222–226 (1996).
14. E. Zielinski, F. Keppler, S. Hausser, M. H. Pilkuhn, R. Sauer, and W. T. Tsang, "Optical gain and loss processes in GaInAs InP MQW laser structures," IEEE J. Quantum Electron. **25**, 1407–1416 (1989).

1. Introduction

Two-dimensional photonic crystal (PC) microcavity lasers [1, 2] would be a more promising source candidate for photonic integrated circuits (PIC) if they were capable of higher output powers and higher output slope efficiencies. Photonic crystal lasers have typically suffered from an absorption loss due to the active medium (quantum wells or quantum dots) in the mirror regions of the cavity where carrier density is below transparency. The threshold gain ($g_{\text{threshold}}$) and slope efficiency (η_{slope}) are expressed as:

$$\Gamma g_{\text{threshold}} = \alpha_{\text{total}} = \alpha_{\text{passive}} + \alpha_{\text{absorption}}, \tag{1}$$

$$\eta_{\text{slope}} = \eta_{\text{collection}}\,\eta_{\text{internal}}\,\frac{\alpha_{\text{passive}}}{\alpha_{\text{passive}} + \alpha_{\text{absorption}}}. \tag{2}$$

where Γ is the confinement factor and α_{total} is the total optical loss which consists of not only loss of a passive resonator but also absorption loss. By reducing this absorption term ($\alpha_{\text{absorption}}$) in Eq. (1) and (2), we can decrease the laser threshold and increase the slope efficiency at the same time.

We have recently demonstrated optically-pumped pulsed output powers of one hundred micro-watts in edge-emitting double-heterostructure (DH) microcavities [3, 4]. These devices could be improved if the absorption due to the quantum wells in the mirror regions was eliminated. In this demonstration we reduce or eliminate this loss by blue-shifting the quantum well absorption peak in the mirror region using quantum well intermixing (QWI). Figure 1 illustrates the device we have in mind. The intermixing was accomplished using the ion implantation approach [5, 6, 7].

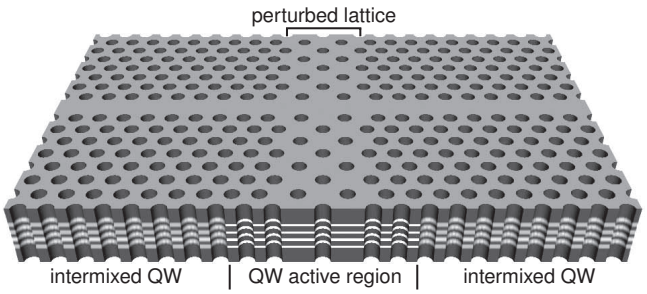

Fig. 1. Schematic illustration of an intermixed DH cavity.

2. Device fabrication

DH [8, 9] photonic crystal lasers were formed in a 240nm thick InGaAsP active waveguide capped by a 60nm InP layer grown by MOCVD on a (100) InP substrate. The active region contains four compressively strained InGaAsP QWs. A 400nm thick silicon nitride (SiN_x) layer was first deposited on the sample and a 35nm thick nickel film of stripe patterns was evaporated on it through lift-off. A wet-etch of the SiN_x followed by removing the nickel film left nitride stripes with different widths. The resulting nitride stripe widths were 1, 2, 3, and 4 microns.

#101315 - $15.00 USD Received 9 Sep 2008; revised 8 Oct 2008; accepted 8 Oct 2008; published 14 Oct 2008

They masked the active regions so that the central areas of the laser cavities would not be disordered. Then a 1×10^{15}cm^{-2} dose of 10keV P+ ions were implanted. During implantation the sample was tilted 7° away from surface normal. Other conditions were a 200 °C substrate temperature and a 100nA/cm^2 current density. The P+ ions stop inside the 60nm InP cap in regions where there was no nitride layer and get completely blocked by the SiN_x stripes [10]. Next, the SiN_x stripes were removed and a 100nm thick e-beam evaporated SiO_2 film was deposited on the sample at a rate of 4Å per second. This was done to protect the surface from decomposition in the subsequent high temperature annealing, which was done at 700 °C for 4 minutes in a nitrogen gas environment in a rapid thermal annealer (RTA). During this anneal, defects inside the InP cap created by implantation propagate down and intermix the four QWs below. The SiO_2 film was then removed and the intermixed sample was ready for patterning PC microcavities. The resonant cavity fabrication followed the same procedures as in Ref. [11] with the addition that during the e-beam lithography step the devices were aligned with respect to nickel alignment marks defined and protected from the beginning of the processing. The alignment was accomplished with better than 0.5μm accuracy. A final HCl wet etch removed the top InP cap and undercut the QW membrane to form an air bridge. For comparison, every lithography window had an identical array of cavities written in an area that was protected by SiN_x, thus having no intermixing.

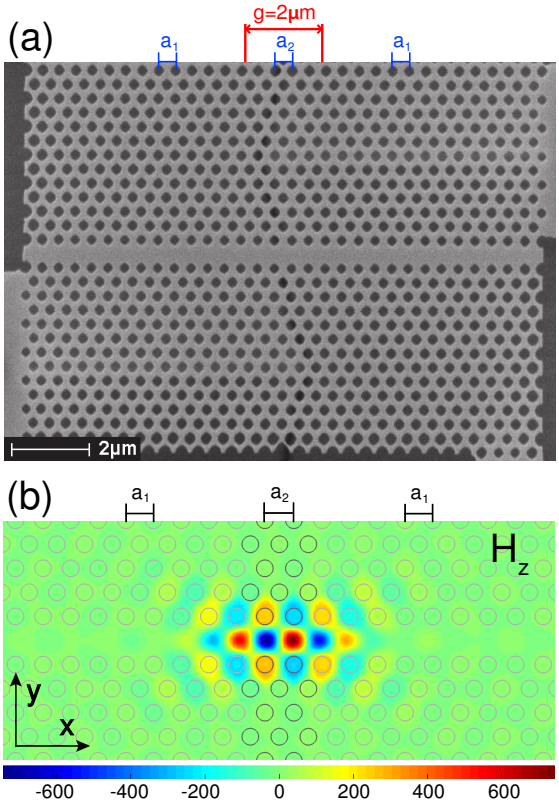

Fig. 2. (color) (a)Top view SEM image of a fabricated intermixed PC DH cavity. Its QW active region (g) after intermixing is illustrated on top. (b)H_z field component of the DH high-Q mode at the mid-plane of the membrane calculated by 3D FDTD. Air holes are outlined in gray and the perturbed center defect lattices are in darker gray. In both Fig. 2(a) and 2(b), a_2 is 5% larger than a_1.

#101315 - $15.00 USD Received 9 Sep 2008; revised 8 Oct 2008; accepted 8 Oct 2008; published 14 Oct 2008

Figure 2(a) shows the top view of a finished PC DH cavity. The lattice constant in the waveguide cladding region, a_1, is 420nm and the lattice constant in the center perturbed area, a_2, is 5% larger along the waveguide direction only. The hole radius to lattice constant ratio, r/a_1, is approximately 0.31. The upper section of Fig. 2(a) indicates the region (g) that was protected by the nitride mask and not subsequently intermixed. This two micron stripe indicated in the figure runs perpendicular to the waveguide axis of the DH resonant cavity.

The field profile of the high-Q DH mode is shown in Fig. 2(b). A passive quality factor (Q) of 265,000 is obtained from three-dimensional (3D) finite-difference-time-domain (FDTD) calculation. The details of the modeling is reported elsewhere [8]. Fig. 2 (a) and (b) shows that most of the field intensity is still within the gain stripe (g) while the QW region overlapping the tail of the mode was intermixed.

3. Results of quantum well intermixing

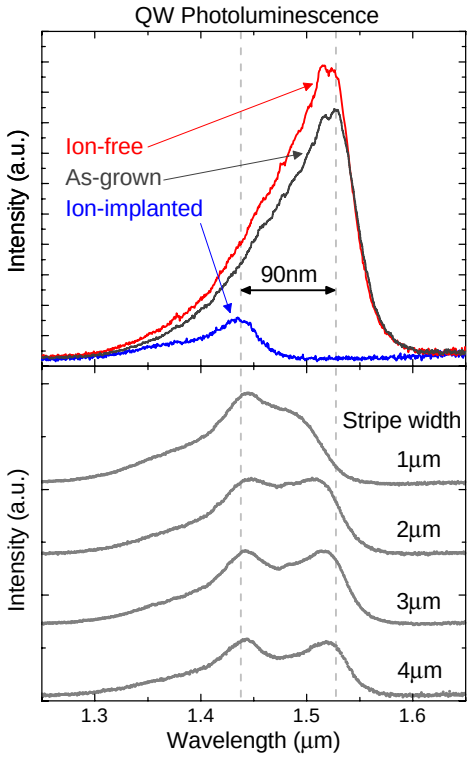

Fig. 3. (color) PL spectra taken at different regions on the QW sample. (a)PL spectra of ion-implanted and ion-free QW regions after annealing, compared with PL of an as-grown QW reference sample under the same experimental condition. (b)PL taken at the transition regions of gain stripes with different width.

Photoluminescence (PL) measurements were first done to check the intermixing results and the resulting spectra are plotted in Fig. 3(a). In the regions where the sample surface was exposed during ion implantation, the PL peak is blue-shifted about 90nm with respect to the area where ions were blocked by the SiN_x. The PL intensity in the intermixed area is also eight times smaller. This is attributed to defects introduced into the QW along with the intermixing. This 90nm PL shift provides a window in wavelength in the 1.55μm band for lasers to operate with

#101315 - $15.00 USD Received 9 Sep 2008; revised 8 Oct 2008; accepted 8 Oct 2008; published 14 Oct 2008

only a narrow active region inside the cavities. It is worth noticing that the PL in the ion-free region has no obvious blue-shifting and its intensity is slightly higher compared to the PL of as-grown QW. This is attributed to defects formed during growth being annealed away.

PL in Fig. 3(b) was taken close to the interfaces of the gain stripes with different widths, so that both peaks can be identified at the same time. The peak separation decreases as the stripe widths narrows because the lateral diffusion of the defects blueshifts the QW in the ion-free stripes and ultimately limits the spatial resolution, which is about 2μm in our process.

4. Improvement in laser thresholds and slope efficiencies

These PC DH cavity pairs (intermixed and non-intermixed) were optically pumped by an 850nm diode laser at normal incidence through a 100$\times$ IR-corrected objective lens at a substrate temperature of 20°C. The pulse duration was 8ns under a 0.1% duty cycle and the pump spot size was about 2μm in diameter. Devices with gain widths, g, of 4, 3 and 2μm all lase. During the measurement, the overlap of the pump spot with the field-confining center region of the DH cavities was optimized while the collection setup was not adjusted. Lasing spectra and input-output characteristics of one device pair (g=2μm) are plotted in Fig. 4. Laser characteristics of three pairs of devices are tabulated in Table. 1.

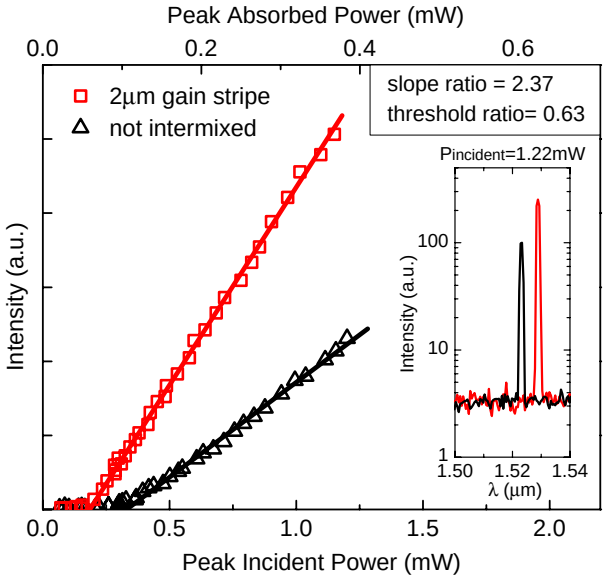

Fig. 4. (color) Light-in-light-out (L-L) curves of the PC DH lasers with 2μm gain stripe and the corresponding non-intermixed reference. Their lasing spectra are shown as inset.

The comparisons from all three pairs of lasers in Table 1. show consistently more than a factor of two increase in the slope efficiencies and a decrease in the threshold pump powers by 20$\sim$37%. All six lasers operate in the wavelength region where the intermixed QW areas are transparent. The slight differences in lasing wavelengths are caused by the slight differences in r/a_1 from device to device. This difference in r/a_1 was verified in SEM images taken of the cavities and is attributed the fact that the two cavity types (disordered and non-disordered) were written at different positions in the field of view during e-beam lithography.

The data collected indicates that by disordering the gain material around the cavity mode, the absorption loss from the gain material can be reduced. The greater than a factor of 2 in-

#101315 - $15.00 USD Received 9 Sep 2008; revised 8 Oct 2008; accepted 8 Oct 2008; published 14 Oct 2008

Table 1. Laser characteristics of three PC DH lasers of different gain stripe widths (g=4, 3, and 2μm) with their non-intermixed references named (g=∞). Their lattice constants (a_1) are 420nm. The ratio is calculated using data from g=4,3,2 over data from g=∞ in the table. r/a_1 is computed through top-view SEM images using an edge detection routine.

g (μm)	r/a_1	λ(nm)	threshold $P_{incident}$ (mW)	threshold ratio	slope ratio
4	0.310	1527.73	0.22	0.80	2.79
∞	0.315	1519.34	0.28		
3	0.302	1539.25	0.19	0.77	2.90
∞	0.307	1531.84	0.25		
2	0.309	1528.60	0.18	0.63	2.37
∞	0.313	1523.21	0.30		

crease in slope efficiencies indicates that more than half of the total loss was eliminated by this disordering. It is still true that absorption loss in the vertical stripe direction still exists.

5. Estimation of laser quality factors

To estimate the quality factor (Q) from our laser thresholds, we apply a simple model described in Ref. [12] to the lasing data of g=3μm laser and its non-disordered pair. We assume an averaged gain region of around 3μm in diameter at the center of the cavities where carriers are uniformly distributed, this leads to an 80% in-plane confinement factor (Γ_{xy}). 40% of the incident power ($P_{incident}$) is calculated to be absorbed by the slab and an 80% internal quantum efficiency ($\eta_{internal}$) [13] is used. The result gives device Q of 5,200 and 15,000 for the non-intermixed and intermixed lasers at their lasing thresholds. This improvement of about 8,000 in Q is due to the reduced absorption loss in the mirror cladding by QW intermixing. The mode energy that overlaps the intermixed QW region is 0.019 of the total energy of the mode, evaluated from the calculated mode profiles. An internal QW absorption coefficient of 1,100cm $^{-1}$ is extracted from this data, which agrees with the reported value [14]. By importing the structure information from the top view SEM image into 3D FDTD calculation, we get a passive device Q of 75,200. This implies equivalent quality factors of 5,600 and 18,700 left for absorption loss in the non-intermixed and intermixed lasers at their thresholds.

6. Conclusion

In summary, we demonstrated PC DH microcavity QW membrane lasers with a significantly reduced absorption loss using a quantum well intermixing technique to disorder the mirror regions. The slope efficiencies of these disordered devices increased by more than a factor of two and the threshold pump powers were reduced by 20% or more. We believe this result is promising for monolithic integration of PC microcavity lasers with passive devices and suggests an interesting route towards better performance of PC microcavity lasers.

Acknowledgments

We thank Stephen Farrell at University of Southern California for his help on fabrication. This study is based on research supported by DARPA under contract No. F49620-02-1-0403 and by NSF under grant ECS-0507270.

#101315 - $15.00 USD Received 9 Sep 2008; revised 8 Oct 2008; accepted 8 Oct 2008; published 14 Oct 2008